Inorg. Chem. **2009**, *48*, 628−637

Syntheses and Crystal Structures of Novel Manganese(II) or Cadmium(II) Arsonates with Dinuclear Clusters or 1D Arrays

Fei-Yan Yi, Na Zhao, Wei Wu, and Jiang-Gao Mao*

State Key Laboratory of Structure Chemistry, Fujian Institute of Research on the Structure of Matter, Chinese Academy of Sciences, Fuzhou 350002, P. R. China

Received August 29, 2008

Hydrothermal reactions of cadmium(II) or manganese(II) salts with aryl arsenic acids $RAsO_3H_2$ ($R = C_6H_5-$, H_2L^1; $3\text{–}NO_2-4\text{–}OH-C_6H_3-$, H_3L^2) and 1,10-phenanthroline (phen) led to six new cadmium(II) and manganese(II) organo arsonates, namely, $Cd(phen)(HL^1)_2(H_2O)$ (**1**), $M(phen)(H_2L^2)_2$ (M = Mn, **2**; Cd, **3**), $[M(phen)_2(H_2L^2)](ClO_4)\cdot(H_2O)$ (M = Mn, **4**; Cd, **5**), and $[Mn(phen)_2(HL^1)](ClO_4)\cdot(H_2O)$ (**6**). The structures of **1**, **4**, and **5** contain two types of dinuclear clusters, whereas **2** and **3** exhibit 1D chains based on dinuclear $M_2(\mu\text{-}O)_2$ cluster units further bridged by arsonate ligands. Compound **6** features a 1D helical chain in which neighboring two metal centers are bridged by one arsonate ligand. Magnetic property measurements on compounds **2**, **4**, and **6** indicate that there exist very weak antiferromagnetic interactions between magnetic centers in all three compounds. Compounds **1**−**6** display typical ligand-centered fluorescence emission bands.

Introduction

The chemistry of metal phosphonates has been an active research area in recent years due to its potential applications in the areas of catalysis, ion exchange, proton conductivity, intercalation chemistry, photochemistry, and materials chemistry.[1,2] Most of metal phosphonates display a layered structure in which the metal centers are bridged by the phosphonate groups, although a variety of 1D chains and porous 3D networks have also been reported.[3] Metal phosphonates containing a molecular cluster unit have been also isolated.[4−10] These 0D compounds are very important; for example, manganese compounds are of great research interest because of their biological relevance as models of active sites in metal enzymes and their unusual magnetic behavior, such as their ability to function as single molecule magnets.[11,12] It is found that minor changes in phosphonate ligands or solvents can lead to completely different cluster cores.

* Author to whom correspondence should be addressed. E-mail: mjg@fjirsm.ac.cn.

(1) (a) Clearfield, A. *Metal Phosphonate Chemistry in Progress in Inorganic Chemistry*; Karlin, K. D., Ed.; John Wiley & Sons: New York, 1998; Vol. *47*, pp 371−510 (and references therein). (b) Mao, J.-G. *Coord. Chem. Rev.* **2007**, *251*, 1493. (c) Matczak-Jon, E.; Videnova-Adrabinska, V. *Coord. Chem. Rev.* **2005**, *249*, 2458.

(2) (a) Cheetham, A. K.; Ferey, G.; Loiseau, T. *Angew. Chem., Int. Ed.* **1999**, *38*, 3268. (b) Zhu, J.; Bu, X.; Feng, P.; Stucky, G. D. *J. Am. Chem. Soc.* **2000**, *122*, 11563. (c) Rao, C. N. R.; Natarajan, S.; Vaidhyanathan, R. *Angew. Chem., Int. Ed.* **2004**, *43*, 1466.

(3) (a) Maeda, K. *Microporous Mesoporous Mater.* **2004**, *73*, 47 (and references therein). (b) Kubicek, V.; Kotek, J.; Hermann, P.; Lukes, I. *Eur. J. Inorg. Chem.* **2007**, 333. (c) Tang, S.-F.; Song, J.-L.; Li, X.-L.; Mao, J.-G. *Cryst. Growth Des.* **2007**, *7*, 360. (d) Konar, S.; Zon, J.; Prosvirin, A. V.; Dunbar, K. R.; Clearfield, A. *Inorg. Chem.* **2007**, *46*, 5229.

(4) (a) Comby, S.; Scopelliti, R.; Imbert, D.; Charbonniere, L.; Ziessel, R.; Bunzli, J.-C. G. *Inorg. Chem.* **2006**, *45*, 3158. (b) Du, Z.-Y.; Xu, H.-B.; Mao, J.-G. *Inorg. Chem.* **2006**, *45*, 9780. (c) Cao, D.-K.; Xiao, J.; Tong, J.-W.; Li, Y.-Z.; Zheng, L.-M. *Inorg. Chem.* **2007**, *46*, 428. (d) Bao, S.-S.; Ma, L.-F.; Wang, Y.; Fang, L.; Zhu, C.-J.; Li, Y.-Z.; Zheng, L.-M. *Chem.−Eur. J.* **2007**, *13*, 2333.

(5) (a) Walawalker, M. G.; Roesky, H. W.; Murugavel, R. *Acc. Chem. Res.* **1999**, *32*, 117 (and references therein). (b) Konar, S.; Clearfield, A. *Inorg. Chem.* **2008**, *47*, 5573. (c) Konar, S.; Clearfield, A. *Inorg. Chem. Commun.* **2008**, *47*, 3489.

(6) (a) Dumas, E.; Sassoye, C.; Smith, K. D.; Sevov, S. C. *Inorg. Chem.* **2002**, *41*, 4029. (b) Langley, S.; Helliwell, M.; Sessoli, R.; J. Teat, S.; Winpenny, R. E. P. *Inorg. Chem.* **2008**, *47*, 497. (c) Breeze, B. A.; Shanmugam, M.; Tuna, F.; Winpenny, R. E. P. *Chem. Commun.* **2007**, 5185. (d) Baskar, V.; Shanmugam, M.; Carolina Sañudo, E.; Shanmugam, M.; Collison, D.; McInnes, E. J. L.; Wei, Q.; Winpenny, R. E. P. *Chem. Commun.* **2007**, 37.

(7) (a) Konar, S.; Bhuvanesh, N.; Clearfield, A. *J. Am. Chem. Soc.* **2006**, *128*, 9604. (b) Tolis, E. I.; Engelhardt, L. P.; Mason, P. V.; Rajaraman, G.; Kindo, K.; Luban, M.; Matsuo, A.; Nojiril, H.; Raftery, J.; Schroder, C.; Timco, G. A.; Tuna, F.; Wernsdorfer, W.; Winpenny, R. E. P. *Chem.−Eur. J.* **2006**, *12*, 8961. (c) Yao, H. C.; Wang, J.-J.; Ma, Y.-S.; Waldmann, O.; Du, W. X.; Song, Y.; Li, Y.-Z.; Zheng, L.-M.; Decurtins, S.; Xin, X.-Q. *Chem. Commun.* **2006**, 1745. (d) Tolis, E. I.; Helliwell, M.; Langley, S.; Raftery, J.; Winpenny, R. E. P. *Angew. Chem., Int. Ed.* **2003**, *42*, 3804. (e) Yao, H. C.; Li, Y.-Z.; Zheng, L.-M.; Xin, X.-Q. *Inorg. Chim. Acta* **2005**, *358*, 2523.

(8) (a) Langley, S. J.; Helliwell, M.; Sessoli, R.; Rosa, P.; Wernsdorfer, W.; Winpenny, R. E. P. *Chem. Commun.* **2005**, 5029. (b) Brechin, E. K.; Coxall, R. A.; Parkin, A.; Parsons, S.; Tasker, P. A.; Winpenny, R. E. P. *Angew. Chem., Int. Ed.* **2001**, *40*, 2700.

10.1021/ic8016535 CCC: $40.75
Published on Web 12/10/2008

Metal arsonates are expected to display a similar structural chemistry to those of metal phosphonates, but the larger ionic radius of As(V) compared to P(V) could lead to some different architectures with different physical properties. So far, reports on metal organo arsonates are very limited.[13−17] A variety of polyoxometalate (POM) clusters of vanadium, molybdenum, and tungsten have been reported,[13−15] in which each arsonate group bridges with several metal centers as the phosphonate group in metal phosphonates containing POM clusters.[18c] It is interesting that, during the investigations of the V/O/$PhAsO_3^{2-}$ system, the condensation of the arsonate ligand gave a new hexadentate ligand, $\{Ph_6As_6O_{14}\}^{4-}$, in addition to the unusual $\{V_2O_3\}^{4+}$ cluster,[16a] and the structure of another vanadium compound, $V_2O_4(PhAsO_3H)\cdot H_2O$, features a vanadium oxide layer, with the arsonate ligand hanging on the interlayer space.[16b] In a gallium compound, two $PhAsO_3^{2-}$ ligands were also condensed into a dimeric $\{Ph_2As_2O_5\}^{2-}$ anion, which bridges with two Ga(III) ions and forms a four-membered ring.[17] Organo oxo tin clusters with organo arsonates have been prepared recently using the solvothermal approach of Ma's group.[19]

There are no structural reports on manganese(II) or cadmium(II) arsonates so far. In order to understand the similarities and differences between later transition metal phosphonates and their arsonates, we selected phenylarsonic acid (H_2L^1) and 4-hydroxy-3-nitrophenylarsonic acid (H_3L^2) as the arsonate ligands and 1,10-phenanthroline as the auxiliary ligand. Hydrothermal reactions of Mn(II) or Cd(II) salts with the above two types of ligands resulted in six new cadmium(II) or manganese(II) organo arsonates, namely, $Cd(phen)(HL^1)_2(H_2O)$ (**1**), $M(phen)(H_2L^2)_2$ (M = Mn, **2**; Cd, **3**), $[M(phen)_2(H_2L^2)](ClO_4)\cdot(H_2O)$ (M = Mn, **4**; Cd, **5**), and $[Mn(phen)_2(HL^1)](ClO_4)\cdot(H_2O)$ (**6**). Herein, we report their syntheses, crystal structures, and magnetic and luminescent properties.

Experimental Section

Materials and Methods. Phenylarsonic acid and 4-hydroxy-3-nitrophenylarsonic acid were purchased from TCI (99%) and Acros (98%), respectively. All other chemicals were obtained from commercial sources and used without further purification. Elemental analyses were performed on a German Elementary Vario EL III instrument. The FT-IR spectra were recorded on a Nicolet Magna 750 FT-IR spectrometer using KBr pellets in the range of 4000−400 cm^{-1}. Thermogravimetric analyses were carried out on a NETZSCH STA 449C unit at a heating rate of 15 °C/min under a nitrogen atmosphere. Powder X-ray diffraction (XRD) patterns (Cu Kα) were collected on an XPERT-MPD θ-2θ diffractometer. Magnetic susceptibility measurements were carried out on a Quantum Design MPMSXL SQUID magnetometer. The raw data were corrected for the susceptibility of the container and the diamagnetic contributions of the sample using Pascal constants. Photoluminescence analyses were performed on a Perkin Elemer LS55 fluorescence spectrometer.

Synthesis of $Cd(phen)(HL^1)_2(H_2O)$ (1). A mixture of $Cd(CH_3COO)_2\cdot 2H_2O$ (0.2 mmol), H_2L^1 (0.4 mmol), and phen (0.4 mmol) in 10 mL of deionized water was sealed into a Parr Teflon-lined autoclave (23 mL) and heated at 165 °C for five days. The initial and final pH values of the solution were 4.0 and 3.5, respectively. The resultant solution was allowed to evaporate slowly at room temperature; colorless cubic crystals of compound **1** were collected in a ca. 81% yield (based on Cd) after four days. Its purity was also confirmed by powder XRD (see the Supporting Information). Elem anal. calcd for $C_{24}H_{22}As_2CdN_2O_7$ (M_r = 712.68): C, 40.45; H, 3.11; N, 3.93%. Found: C, 40.09; H, 3.33; N, 3.74%. IR data (KBr, cm^{-1}): 3412 (w), 3056 (m), 2381 (m), 1622 (w), 1591 (w), 1577 (w), 1516 (m), 1439 (m), 1427 (m), 1346 (w), 1314 (w), 1244 (m), 1186 (w), 1139 (w), 1096 (s), 1052 (w), 876 (vs), 848 (m), 825 (m), 775 (w), 747 (m), 729 (vs), 694 (m), 648 (w), 481 (m), 472 (m), 434 (w).

Syntheses of $M(phen)(H_2L^2)_2$ (M = Mn, 2; Cd, 3). A mixture of $Mn(CH_3COO)_2\cdot 2H_2O$ (0.1 mmol), H_3L^2 (0.2 mmol), and phen (0.1 mmol) in 10 mL of deionized water was put into a Parr Teflon-lined autoclave (23 mL) and heated at 170 °C for three days. The

(9) (a) Chandrasekhar, V.; Kingsley, S. *Angew. Chem., Int. Ed.* **2000**, *39*, 2320. (b) Yang, Y.; Pinkas, J.; Noltemeyer, M.; Schmidt, H.-G.; Roesky, H. W. *Angew. Chem., Int. Ed.* **1999**, *38*, 664. (c) Chandrasekhar, V.; Sasikumar, P.; Boomishankar, R.; Anantharaman, G. *Inorg. Chem.* **2006**, *45*, 3344. (d) Lei, C.; Mao, J.-G.; Sun, Y.-Q.; Zeng, H.-Y.; Clearfield, A. *Inorg. Chem.* **2003**, *42*, 6157. (e) Yang, B.-P.; Mao, J.-G.; Sun, Y.-Q.; Zhao, H.-H.; Clearfield, A. *Eur. J. Inorg. Chem.* **2003**, 4211. (f) Cao, D.-K.; Li, Y.-Z.; Zheng, L.-M. *Inorg. Chem.* **2005**, *44*, 2984. (g) Du, Z.-Y.; Xu, H.-B.; Mao, J.-G. *Inorg. Chem.* **2006**, *45*, 6424.

(10) (a) Maheswaran, S.; Chastanet, G.; Teat, S. J.; Mallah, T.; Sessoli, R.; Wernsdorfer, W.; Winpenny, R. E. P. *Angew. Chem., Int. Ed.* **2005**, *44*, 5044. (b) Shanmugam, M.; Chastanet, G.; Mallah, T.; Sessoli, R.; Teat, S. J.; Timco, G. A.; Winpenny, R. E. P. *Chem.—Eur. J.* **2006**, *12*, 8777. (c) Shanmugam, M.; Shanmugam, M.; Chastanet, G.; Sessoli, R.; Mallah, T.; Wernsdorfe, W.; Winpenny, R. E. P. *J. Mater. Chem.* **2006**, *16*, 2576. (d) Yao, H.-C.; Li, Y.-Z.; Song, Y.; Ma, Y.-S.; Zheng, L.-M.; Xin, X.-Q. *Inorg. Chem.* **2006**, *45*, 59.

(11) (a) Pecoraro, V. L. *Manganese Redox Enzymes*; VCH: Weinheim, Germany, 1992. (b) Ferreira, K. N.; Iverson, T. M.; Maghlaoui, K.; Barber, J.; Iwata, S. *Science* **2004**, *303*, 1831. (c) Mishra, A.; Wernsdorfer, W.; Abboud, K. A.; Christou, G. *Chem. Commun.* **2005**, 54.

(12) (a) Sessoli, R.; Gatteschi, D.; Caneschi, A.; Novak, M. A. *Nature* **1993**, *365*, 141. (b) Aubin, S. M. J.; Dilley, N. R.; Wemple, M. W.; Maple, M. B.; Christou, G.; Hendrickson, D. N. *J. Am. Chem. Soc.* **1998**, *120*, 839. (c) Gatteschi, D.; Sessoli, R. *Angew. Chem., Int. Ed.* **2003**, *42*, 268.

(13) (a) Burkholder, E.; Zubieta, J. *Inorg. Chim. Acta* **2004**, *357*, 301. (b) Burkholder, E.; Wright, E.; Golub, V.; O'Connor, C. J.; Zubieta, J. *Inorg. Chem.* **2003**, *42*, 7460. (c) Barkigia, K. M.; Rajkovic-Blazer, L. M.; Pope, M. T.; Quicksall, C. O. *Inorg. Chem.* **1981**, *20*, 3318. (d) Johnson, B. J. S.; Geers, S. A.; Brennessel, W. W.; Young, V. G., Jr.; Stein, A. *Dalton Trans.* **2003**, 4678. (e) Liu, B.; Ku, Y.; Wang, M.; Zheng, P. *Inorg. Chem.* **1988**, *27*, 3868.

(14) (a) Matsumoto, K. Y. *Bull. Chem. Soc. Jpn.* **1978**, *51*, 492. (b) Liu, B.-Y.; Xie, G.-Y.; Ku, Y.-T.; Wang, X. *Polyhedron* **1990**, *9*, 2023. (c) Khan, M. I.; Zubieta, J. *Angew. Chem., Int. Ed.* **1994**, *33*, 760. (d) Khan, M. I.; Chang, Y.; Chen, Q.; Hope, H.; Parking, S.; Goshorn, D. P.; Zubieta, J. *Angew. Chem., Int. Ed.* **1992**, *31*, 1197. (e) Johnson, B. J. S.; Schroden, R. C.; Zhu, C.; Young Junior, V. G.; Stein, A. *Inorg. Chem.* **2002**, *41*, 2213.

(15) (a) Kwak, W.; Rajkovic, L. M.; Stalick, J. K.; Pope, M. T.; Quicksall, C. O. *Inorg. Chem.* **1976**, *15*, 2778. (b) Chang, Y.-D.; Zubieta, J. *Inorg. Chim. Acta* **1996**, *245*, 177. (c) Johnson, B. J. S.; Schroden, R. C.; Zhu, C.; Stein, A. *Inorg. Chem.* **2001**, *40*, 5972. (d) Liu, B.-Y.; Ku, Y.-T.; Wang, X. *Inorg. Chim. Acta* **1989**, *161*, 233.

(16) (a) Salta, J.; Chang, Y.-D.; Zubieta, J. J. *Chem. Soc., Chem. Commun.* **1994**, 1039. (b) Huan, G.; Johnson, J. W.; Jacobson, A. J.; Merola, J. S. *Chem. Mater.* **1990**, *2*, 719.

(17) Mason, M. R.; Mattews, R. M.; Mashuta, M. S.; Richardson, J. F.; Vij, A. *Inorg. Chem.* **1997**, *36*, 6476.

(18) (a) Zhang, X. M.; Hou, J. J.; Zhang, W. X.; Chen, X. M. *Inorg. Chem.* **2006**, *45*, 8120. (c) Burkholder, E.; Golub, V.; O'Connor, C. J.; Zubieta, J. *Inorg. Chem.* **2004**, *43*, 7014. (d) Lin, C. H.; Lii, K. H. *Inorg. Chem.* **2004**, *43*, 6403. (e) Murugavel, R.; Shanmugan, S. *Chem. Commun.* **2007**, 1257.

(19) Xie, Y. P.; Yang, J.; Ma, J. F.; Zhang, L. P.; Song, S. Y.; Su, Z. M. *Chem.—Eur. J.* **2008**, *14*, 4093.

Table 1. Summary of Crystal Data and Structure Refinements for **1**−**6**

compounds	**1**	**2**	**3**	**4**	**5**	**6**
formula	$C_{24}H_{22}As_2CdN_2O_7$	$C_{24}H_{18}As_2MnN_4O_{12}$	$C_{24}H_{18}As_2CdN_4O_{12}$	$C_{30}H_{23}AsClMnN_5O_{11}$	$C_{30}H_{23}AsCdClN_5O_{11}$	$C_{30}H_{24}AsClMnN_4O_8$
fw	712.68	759.20	816.66	794.84	852.30	733.84
space group	$P\bar{1}$	$P2_1/c$	$P\bar{1}$	$P\bar{1}$	$P\bar{1}$	$P2_1/n$
a (Å)	8.9177(5)	8.182(3)	8.315(6)	9.793(6)	10.055(4)	13.804(5)
b (Å)	12.1601(7)	15.023(6)	15.00 (1)	12.988(8)	12.654(5)	8.326(3)
c (Å)	12.5849(7)	21.080(9)	21.26 (1)	13.758(8)	13.629(5)	27.13 (1)
α (deg)	67.840 (1)	90	90	113.872(5)	111.839(4)	90
β (deg)	85.72	91.346(6)	90.41 (1)	92.578(6)	92.554 (1)	102.496(5)
γ (deg)	83.217 (1)	90	90	102.305(6)	101.575(5)	90
V (Å^3)	1254.4(1)	2590 (1)	2652(3)	1547(1)	1563 (1)	3044 (1)
Z	2	4	4	2	2	4
D_{calcd} (g cm^{-3})	1.887	1.947	2.045	1.707	1.811	1.601
μ (mm^{-1})	3.536	3.122	3.375	1.647	1.905	1.658
GOF	1.127	1.096	1.147	1.035	1.048	1.067
R_1, wR_2 [$I > 2\sigma(I)$][a]	0.0254, 0.0598	0.0619, 0.1161	0.0655, 0.1189	0.0590, 0.1185	0.0447, 0.0927	0.0752, 0.1584
R_1, wR_2 (all data)	0.0304, 0.0645	0.0853, 0.1269	0.0905, 0.1309	0.1004, 0.1435	0.0618, 0.1019	0.1238, 0.1835

[a] $R_1 = \sum||F_o| - |F_c||/\sum|F_o|$, $wR_2 = \{\sum w[(F_o)^2 - (F_c)^2]^2/\sum w[(F_o)^2]^2\}^{1/2}$.

initial and final pH values of the solution were 2.5 and 3.0, respectively. Yellow needle crystals of **2** and **3** were collected in about 45% yield based on Mn or Cd. Their purities were also confirmed by powder XRD (see the Supporting Information). Elem anal. calcd for $C_{24}H_{18}As_2MnN_4O_{12}$ (M_r = 759.20): C, 37.97; H, 2.39; N, 7.38%. Found: C, 37.80; H, 2.46; N, 7.33%. Elem anal. calcd for $C_{24}H_{18}As_2CdN_4O_{12}$ (M_r = 816.66): C, 35.30; H, 2.22; N, 6.86%. Found: C, 34.26; H, 3.13; N, 6.69%. IR data (KBr, cm^{-1}) for **2**: 3434 (w), 3288 (m), 3058 (m), 2724 (w), 2310 (w) 1618 (s), 1579 (m), 1568 (m), 1536 (s), 1519 (w), 1479 (m), 1426 (s), 1350 (m), 1332 (m), 1319 (m), 1281 (w), 1252 (s), 1201 (m), 1148 (w), 1137 (w), 1101 (w), 1076 (m), 921 (s), 899 (s), 845 (s), 813 (m), 783 (w), 753 (s), 731 (m), 635 (w), 551 (s). IR data (KBr, cm^{-1}) for **3**: 3427 (m), 3286 (w), 3060 (w), 2918 (w), 2396 (w), 1616 (s), 1578 (w), 1532 (s), 1479 (w), 1428 (m), 1347 (m), 1318 (s), 1254 (s), 1199 (w), 1147 (m), 1101 (m), 1078 (m), 914 (w), 867 (s), 845 (s), 765 (m), 752 (w), 729 (m), 550 (s).

Syntheses of [M(phen)$_2$(H$_2$L^2)](ClO$_4$)·(H$_2$O) (M = Mn, 4; Cd, 5). Compound **4** was obtained by hydrothermal reaction of a mixture of $Mn(ClO_4)_2$ (0.3 mmol), H_3L^2 (0.2 mmol), and phen (0.1 mmol) in 10 mL of deionized water with an initial pH value of about 3.0 at 170 °C for two days, whereas compound **5** was prepared by hydrothermal reaction of $Cd(NO_3)_2 \cdot 6H_2O$, $Cd(ClO_4)_2$, H_3L^2, and phen in a 1:2:1:1 molar ratio at 120 °C for five days. Efforts to use $Cd(ClO_4)_2$ as the only metal source were tried but were unsuccessful. We still do not know the role of the nitrate anion in the crystallization of compound **5**. Yellow prism-shaped crystals of **4** and **5** were collected in about 50% yield for **4** and 15% for yield **5** (based on phen). The purity for **4** was also confirmed by powder XRD (see the Supporting Information). Elem anal. calcd for $C_{30}H_{23}AsClMnN_5O_{11}$ (M_r = 794.84): C, 45.33; H, 2.92; N, 8.81%. Found: C, 44.81; H, 2.90; N, 8.75%. Elem anal. calcd for $C_{30}H_{23}AsClCdN_5O_{11}$ (M_r = 852.30): C, 42.28; H, 2.72; N, 8.22%. Found: C, 42.20; H, 2.68; N, 8.19%. IR data for **4** (KBr, cm^{-1}): 3736 (w), 3540 (w), 3286 (w), 3066 (w), 2972 (w), 1616 (s), 1591 (m), 1570 (m), 1531 (m), 1518 (s), 1477 (m), 1425 (s), 1323 (m), 1254 (m), 1224 (w), 1185 (w), 1144 (m), 1102 (vs), 1077 (s), 918 (s), 897 (w), 864 (w), 845 (s), 765 (w), 729 (s), 623 (m), 549 (m). IR data (KBr, cm^{-1}) for **5**: 3513 (m), 3293 (m), 3074 (m), 3011 (w), 2412 (w), 1997 (w), 1811 (w), 1617 (s), 1592 (m), 1575 (m), 1531 (m), 1518 (s), 1476 (m), 1451 (w), 1428 (s), 1344 (m), 1325 (s), 1253 (s), 1224 (w), 1189 (w), 1146 (m), 1099 (vs), 908 (s), 848 (vs), 766 (m), 749 (m), 728 (s), 624 (s), 549 (m).

Synthesis of [Mn(phen)$_2$(HL^1)](ClO$_4$)·(H$_2$O) (6). A mixture of $Mn(ClO_4)_2$ (0.2 mmol), H_2L^1 (0.2 mmol), and phen (0.2 mmol) in 10 mL of deionized water with an initial pH value of about 3.5 was put into a Parr Teflon-lined autoclave (23 mL) and heated at 120 °C for five days. Yellow prism-shaped crystals of compound **6** were collected in about 65% yield for **6** (based on phen). The purity for **6** was also confirmed by XRD powder diffraction (see the Supporting Information). Elem anal. calcd for $C_{30}H_{24}AsClMnN_4O_8$ (M_r = 733.84): C, 49.10; H, 3.30; N, 7.63%. Found: C, 49.69; H, 3.17; N, 7.70%. IR data (KBr, cm^{-1}): 3444 (s), 3077 (w), 2929 (w), 2361 (w), 1624 (m), 1591 (w), 1578 (w), 1517 (s), 1495 (w), 1440 (w), 1424 (s), 1342 (w), 1225 (w), 1144 (m), 1094 (vs), 897 (w), 875 (w), 858 (m), 843 (s), 724 (s), 691 (m), 639 (m), 623 (s), 470 (w).

Single-Crystal Structure Determination. Data collections were performed on a Saturn 70 CCK diffractometer (for **2**, **3**, **5**, and **6**), a Siemens Smart CCD (for **1**), and a Rigaku Mercury CCD diffractometer (for **4**). All diffractometers were equipped with graphite-monochromated Mo Kα radiation (λ = 0.71073 Å). Intensity data for all six compounds were collected by the narrow frame method at 293 K. The data sets were corrected for Lorentz and polarization factors as well as for absorption by a multiscan method (for **2**−**6**) or Ψ-scan technique (for **1**).[20] All six structures were solved by the direct methods and refined by full-matrix least-squares fitting on F^2 by SHELX-97.[20] All non-hydrogen atoms were refined with anisotropic thermal parameters. C(25), C(26), C(27), C(28), C(29), C(30), N(5), O(4), O(5), and O(6) of **5** are severely disordered, and each displays two orientations with an occupancy factor of 50% for each site. All hydrogen atoms were located at geometrically calculated positions and refined with isotropic thermal parameters. Crystallographic data and structural refinements for compounds **1**−**6** are summarized in Table 1. Important bond lengths are listed in Table 2. More details on the crystallographic studies as well as atomic displacement parameters are given as Supporting Information.

Results and Discussion

Hydrothermal reactions of manganese(II) or cadmium(II) salts with phenylarsonic (H_2L^1) or 4-hydroxy-3-nitrophenylarsonic acid (H_3L^2) and 1,10-phenanthroline (phen) afforded six new transition metal phenylarsonates, namely, Cd(phen)(HL^1)$_2$(H$_2$O) (**1**), M(phen)(H$_2$L^2)$_2$ (M = Mn, **2**; Cd, **3**), [M(phen)$_2$(H$_2$L^2)](ClO$_4$)·(H$_2$O) (M = Mn, **4**; Cd, **5**), and

(20) (a) Sheldrick, G. M. *Program SADABS*; Universität Göttingen: Göttingen, Germany, 1995. (b) *CrystalClear*, version 1.3.5; Rigaku Corp.: Woodlands, TX, 1999. (c) Sheldrick, G. M. *SHELX-96*; Bruker: Madison, WI, 1996.

Scheme 1. Coordination Modes of H_2L^1 and H_3L^2 ligands in compounds **1** (a), **2** and **3** (b), **4** and **5** (c), and **6** (d)

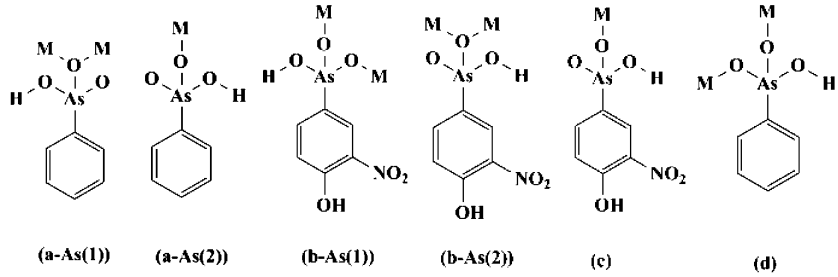

$[Mn(phen)_2(HL^1)](ClO_4)\cdot(H_2O)$ (**6**). They represent the first structurally characterizated Cd(II) or Mn(II) organo-arsenates.

Compound **1** was obtained simply by the evaporation of the resultant solution from hydrothermal reactions at room temperature. When the H_2L^1 ligand was replaced by H_3L^2, $M(phen)(H_2L^2)_2$ (M= Mn, **2**; Cd, **3**) was isolated. Compounds **1**−**3** can also be prepared by using other metal salts such as nitrates or chlorides instead of acetates, but the crystallinity of the products is much poorer and yields are slightly lower. Using $M(ClO_4)_2$ instead of $M(CH_3COO)_2$ led to the isolation of compounds **4**−**6**.

Structure of $Cd(phen)(HL^1)_2(H_2O)$ (1). The structure of compound **1** features an isolated dimeric $[Cd_2(phen)_2(HL^1)_4(H_2O)_2]$. There is one unique cadmium(II) ion in the asymmetric unit of **1** (Figure 1). It is octahedrally coordinated by three phenylarsonate oxygen atoms from three H_2L^1 anions, one bidentate chelating phen ligand, and an aqua ligand. The Cd−O and Cd−N distances are in the range of 2.200(2)−2.357(2) Å and 2.352(3)−2.365(3) Å, respectively, which are comparable to those reported in other cadmium(II) phosphonates.[21,22]

There are two unique H_2L^1 ligands in **1**. Both arsenate groups are singly protonated, as indicated by the elongated As−O bonds (Table 2). However, they show different coordination modes (Scheme 1). The phenylarsonate ligand containing As(1) is bidentate and bridges with two Cd(II) ions via one of three phenylarsonate oxygen atoms (O(2); Scheme 1a-As1). The phenylarsonate ligand containing As(2) is monodentate and connects with a Cd(II) center by using one of its phenylarsonic oxygen atoms (O(4); Scheme 1a-As(2)). A pair of Cd(II) ions are bridged by a pair of arsonate oxygen atoms into a $[Cd_2(phen)_2(HL^1)_4(H_2O)_2]$ dinuclear unit with a Cd_2O_2 four-member ring. The large hindrance effects of phen and the phenyl ring prevents the compound from forming an infinite skeleton.

These discrete dinuclear clusters in **1** are assembled into a complicated 3D network via hydrogen bonds as well as $\pi\cdots\pi$ interactions (Table 2, Figure 2). A number of hydrogen bonds are formed among aqua ligands and noncoordinated phenylarsonate oxygen atoms with O···O separations in the range of 2.619(3)−2.714(4) Å. The $\pi\cdots\pi$ packing interactions occurred between the phenyl of the arsonate ligand (C(1), C(2), C(3), C(4), C(5), and C(6)) and the phenyl ring of the phen ligand (C(23), C(24), C(25), C(26), C(30), and C(31)) with an inter-ring distance of 3.613 Å and a dihedral angle of 2.4 °, as well as between the phenyl ring and pyridyl ring of two neighboring phen ligands with an inter-ring distance of 3.629 Å and a dihedral angle of 0.9 °.

It is interesting to compare the structure of **1** with that of cadmium(II) phenylphosphonates. In the layered $Cd(O_3PC_6H_5)(H_2O)$, the phenylphosphonate is fully deprotonated, and it adopts a pentadentate chelating and bridging coordination mode, chelating bidentately with a Cd(II) ion and bridging with three other ones. The cadmium(II) ion is octahedrally coordinated by five phosphonate oxygen atoms from four phosphonate ligands and an aqua ligand.[23a] When cadmium(II) chloride was allowed to react with the phenylphosphonate ligand and phen in a 1:1:2 molar ratio at 80°, slow evaporation of the resultant solution afforded $[Cd(phen)_3]\cdot C_6H_5PO_3H\cdot Cl\cdot 7H_2O$,[23b] in which the cadmium(II) ion is octahedrally coordinated by three bidentate chelating phen ligands to form a $[Cd(phen)_3]^{2+}$ cation. The phenylphosphonate ligand remains noncoordinated and involves in hydrogen bonding.

Structure of $M(phen)(H_2L^2)_2$ (M = Mn, 2; Cd, 3). Compounds **2** and **3** are isostructural; hence, only the structure of **2** will be discussed in detail as a representative. There is one manganese(II) ion, one phen ligand, and two arsonate anions in the asymmetric unit of **2** (Figure 3). The metal ion is octahedrally coordinated by four phenylarsonic oxygen atoms from four $\{H_2L^2\}^-$ anions and a bidentate-chelating phen ligand. The Mn−O (2.101(4)−2.226(4) Å) and Mn−N (2.331(4)−2.339(4) Å) distances are comparable to those reported in other manganese(II) phosphonates.[24]

Similar to those in compound **1**, the arsenate groups of both $\{H_2L^2\}^-$ anions are singly protonated, as indicated by elongated As−O bonds (Table 2), and both the nitro group

(21) (a) Sharma, C. V. K.; Clearfield, A. *J. Am. Chem. Soc.* **2000**, *122*, 1558. (b) Mao, J.-G.; Wang, Z.; Clearfield, A. *Inorg. Chem.* **2002**, *41*, 3713. (c) Du, Z.-Y.; Li, X.-L.; Liu, Q. Y.; Mao, J.-G. *Cryst. Growth Des.* **2007**, *7*, 1501. (d) Jokiniemi, J.; Vuokila-Laine, E.; Peraniemi, S.; Vepsalainen, J. J.; Ahlgren, M. *CrystEngComm* **2007**, *9*, 158. (e) Cao, D.-K.; Xiao, J.; Li, Y.-Z.; Clemente-Juan, J. M.; Coronado, E.; Zheng, L.-M. *Eur. J. Inorg. Chem.* **2006**, 1830. (f) Wu, J.; Song, Y.-L.; Zhang, E.-P.; Hou, H.-W.; Fan, Y.-T.; Zhu, Y. *Chem.*−*Eur. J.* **2006**, *12*, 5823.

(22) (a) Anantharaman, G.; Walawalkar, M. G.; Murugavel, R.; Gabor, B.; Herbst-Irmer, R.; Baldus, M.; Angerstein, B.; Roesky, H. W. *Angew. Chem., Int. Ed.* **2003**, *42*, 4482. (b) Bakhmutova-Albert, E. V.; Bestaoui, N.; Bakhmutov, V. I.; Clearfield, A.; Rodriguez, A. V.; Llavona, R. *Inorg. Chem.* **2004**, *43*, 1264. (c) Paz, F. A. A.; Shi, F.-N.; Klinowski, J.; Rocha, J.; Trindade, T. *Eur. J. Inorg. Chem.* **2004**, 2759. (d) Cao, D.-K.; Li, Y.-Z.; Song, Y.; Zheng, L.-M. *Inorg. Chem.* **2005**, *44*, 3599. (e) Zhang, X.-M.; Fang, R.-Q.; Wu, H.-S. *Cryst. Growth Des.* **2005**, *5*, 1335.

(23) (a) Cao, G.; Lynch, V. M.; Yacullo, L. N. *Chem. Mater.* **1993**, *5*, 1000. (b) Yang, J.; Ma, J.-F.; Zheng, G.-L.; Li, L.; Li, F.-F.; Zhang, Y.-M.; Liu, J.-F. *J. Solid State Chem.* **2003**, *174*, 116.

Table 2. Selected Bond Lengths (Å) for Compounds **1**−**6**[a]

		Compound **1**	
Cd(1)−O(4)	2.200(2)	Cd(1)−N(2)	2.352(3)
Cd(1)−O(2)#1	2.296(2)	Cd(1)−O(1W)	2.357(2)
Cd(1)−O(2)	2.298(2)	Cd(1)−N(1)	2.365(3)
As(1)−O(3)	1.663(2)	As(2)−O(4)	1.656(2)
As(1)−O(2)	1.675(2)	As(2)−O(6)	1.669(2)
As(1)−O(1)	1.717(2)	As(2)−O(5)	1.732(2)
		hydrogen bonds	
O(1)···O(3)#2	2.619(3)	O(5)···O(6)#3	2.624(3)
O(1W)···O(3)#1	2.714(4)	O(1W)···O(6)	2.682(3)
O(1)−H(1A)···O(3)#2	176.1	O(5)−H(5A)···O(6)#3	174.4
O(1W)−H(1WB)···O(3)#1	167(4)	O(1W)−H(1WA)···O(6)	165(4)
		Compound **2**	
Mn(1)−O(11)#1	2.101(4)	Mn(1)−O(23)#2	2.226(4)
Mn(1)−O(13)	2.166(4)	Mn(1)−N(4)	2.331(4)
Mn(1)−O(23)	2.220(3)	Mn(1)−N(3)	2.339(4)
As(1)−O(11)	1.643(3)	As(2)−O(22)	1.647(3)
As(1)−O(13)	1.661(4)	As(2)−O(23)	1.684(3)
As(1)−O(12)	1.715(4)	As(2)−O(21)	1.718(4)
		hydrogen bonds	
O(1)···O(3)	2.620(8)	O(12)···O(22)#3	2.567(5)
O(4)···O(5)	2.552(7)	O(21)···O(13)	2.581(5)
O(1)−H(1A)···O(3)	140.4	O(12)−H(12A)···O(22)#3	166.0
O(4)-H(4A)···O(5)	142.9	O(21)−H(21A)···O(13)	175.1
		Compound **3**	
Cd(1)−O(11)#1	2.215(5)	Cd(1)−O(13)	2.290(5)
Cd(1)−O(23)	2.313(5)	Cd(1)−O(23)#2	2.343(4)
Cd(1)−N(4)	2.375(6)	Cd(1)−N(3)	2.396(5)
As(1)−O(11)	1.642(5)	As(1)−O(13)	1.663(4)
As(1)−O(12)	1.714(5)	As(2)−O(22)	1.649(5)
As(2)−O(23)	1.671(4)	As(2)−O(21)	1.723(5)
		hydrogen bonds	
O(1)···O(3)	2.634(11)	O(12)···O(22)#3	2.558(7)
O(4)···O(5)	2.574(9)	O(21)···O(13)	2.572(7)
O(1)−H(1A)···O(3)	139.0	O(12)−H(12A)···O(22) #3	163.0
O(4)−H(4A)···O(5)	142.4	O(21)−H(21A)···O(13)	177.2
		Compound **4**	
Mn(1)−O(1)	2.077(3)	Mn(1)−O(2)#1	2.141(3)
Mn(1)−N(1)	2.257(4)	Mn(1)−N(3)	2.284(4)
Mn(1)−N(2)	2.314(4)	Mn(1)−N(4)	2.348(4)
As(1)−O(1)	1.640(3)	As(1)−O(2)	1.660(3)
As(1)−O(3)	1.717(3)		
		hydrogen bonds	
O(6)···O(5)	2.605(6)	O(3)···O(1W)	2.628(5)
O(1W)···O(12)	2.781(7)	O(1W)···O(2)#2	2.823(5)
O(6)−H(6B)···O(5)	140.0	O(3)−H(3B)···O(1W)	158.3
O(1W)−H(1WA)···O(12)	168.5	O(1W)−H(1WB)···O(2) #2	169.4
		Compound **5**	
Cd(1)−O(1)	2.223(3)	Cd(1)−O(2)#1	2.263(3)
Cd(1)−N(1)	2.346(3)	Cd(1)−N(2)	2.392(3)
Cd(1)−N(3)	2.363(3)	Cd(1)−N(4)	2.433(3)
As(1)−O(1)	1.651(3)	As(1)−O(2)	1.664(3)
As(1)−O(3)	1.718(3)		
		hydrogen bonds	
O(6)···O(5)	2.564(11)	O(6′)···O(4′)	2.620(16)
O(3)···O(1W)	2.625(4)	O(1W)···O(12)	2.759(6)
O(1W)···O(2)#2	2.811(4)		
O(6)−H(6B)···O(5)	141.2	O(6′)−H(6′A)···O(4′)	140.8
O(3)−H(3B)···O(1W)	162.4	O(1W)−H(1WA)···O(12)	164.5
O(1W)−H(1WB)···O(2)#2	168.1		
		Compound **6**	
Mn(1)−O(1)#1	2.151(4)	Mn(1)−O(3)	2.153(4)
Mn(1)−N(3)	2.257(5)	Mn(1)−N(1)	2.280(5)
Mn(1)−N(4)	2.279(5)	Mn(1)−N(2)	2.281(5)
As(1)−O(1)	1.658(4)	As(1)−O(3)	1.667(4)
As(1)−O(2)	1.721(4)		

[a] Symmetry transformations used to generate equivalent atoms. For **1**: (#1) $-x+1, -y+2, -z+1$; (#2) $-x+2, -y+2, -z+1$; (#3) $-x+1, -y+2, -z$. For **2** and **3**: (#1) $-x, -y, -z+1$; (#2) $-x+1, -y, -z+1$; (#3) $x-1, y, z$. For **4** and **5**: (#1) $-x-1, -y+1, -z+1$; (#2) $-x-2, -y+1, -z+1$. For **6**: (#1) $-x+3/2, y+1/2, -z+1/2$.

and hydroxyl groups of $\{H_2L^2\}^-$ anions remain noncoordinated. The two $\{H_2L^2\}^-$ anions adopt two different coordination modes (Scheme 1b). The one containing As(2) is bidentate bridging by using one of its three arsonate oxygen atoms (O(23); Scheme 1b-As(2)). The one containing As(1) is also bidentate bridging by using two of its three arsonate oxygen atoms (O(11) and O(13); Scheme 1b-As(2)). A pair of manganese(II) ions is bridged by a pair of As(2)O_3 groups

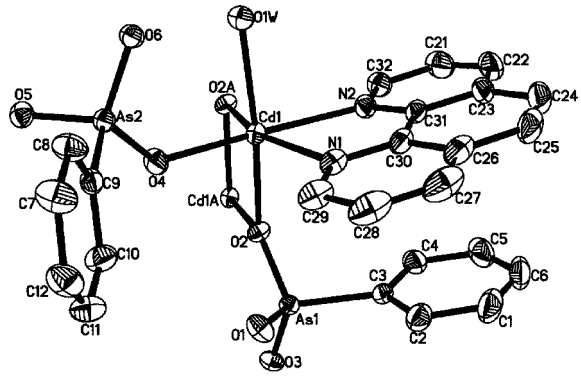

Figure 1. ORTEP representation of the selected unit in compound **1**. The thermal ellipsoids are drawn at 50% probability level. Symmetry code for the generated atoms: (a) $-x + 1, -y + 2, -z + 1$.

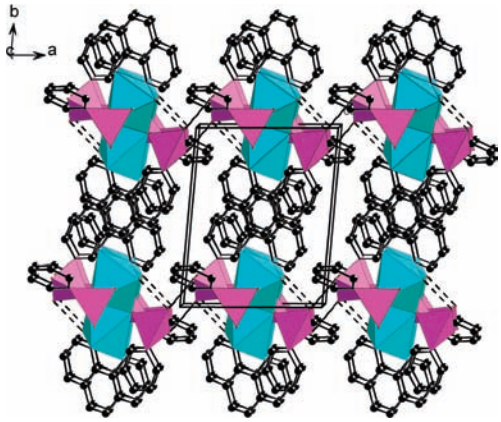

Figure 2. View of the structure of compound **1** down the *c* axis. The CdO_4N_2 octahedra are shaded in cyan, and the $CAsO_3$ tetrahedra are shaded in purple. O and C atoms are drawn as red and black circles, respectively. Hydrogen bonds are represented by dashed lines.

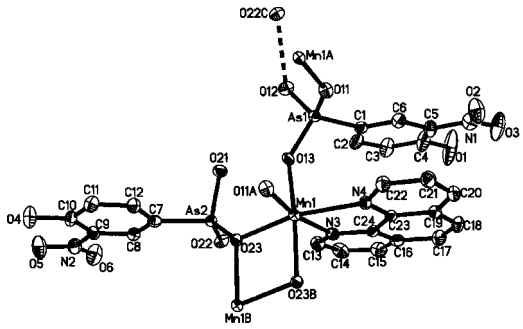

Figure 3. ORTEP representation of the selected unit in compound **2**. The thermal ellipsoids are drawn at the 30% probability level. Symmetry codes for the generated atoms: (a) $-x, -y, -z + 1$; (b) $-x + 1, -y, -z + 1$; (c) $x - 1, y, z$.

into a $[Mn_2(phen)_2(H_2L^2)_2]$ dinuclear unit with a Mn···Mn separation of 3.421(1) Å (Figure 4). Two such neighboring dinuclear units are further bridged by a pair of $As(1)O_3$ groups into a 1D chain, forming Mn_2As_2 four-member rings (Figure 4). The Mn···Mn separation within the Mn_2As_2 ring (Mn−O−As−O−Mn bridge) of 5.210(1) Å is much larger than that of a Mn−O−Mn bridge (3.421(1) Å; Figure 4). Within the 1D chain, the above two types of Mn···Mn separations are alternating. Furthermore, intrachain hydrogen bonds are formed among noncoordination oxygen atoms from arsonate and nitro as well as hydroxyl groups (Figure 4). These 1D metal arsonate chains are further assembled into

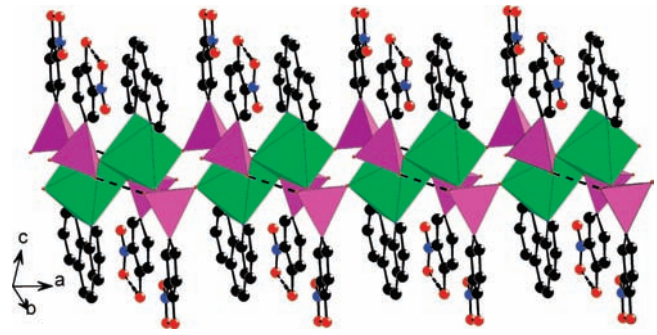

Figure 4. View of the 1D manganese arsonate chain in compound **2**. The MnO_4N_2 octahedra and $CAsO_3$ tetrahedra are shaded in green and purple, respectively. N, O, and C atoms are drawn as blue, red, and black circles, respectively. Hydrogen bonds are drawn as dashed lines.

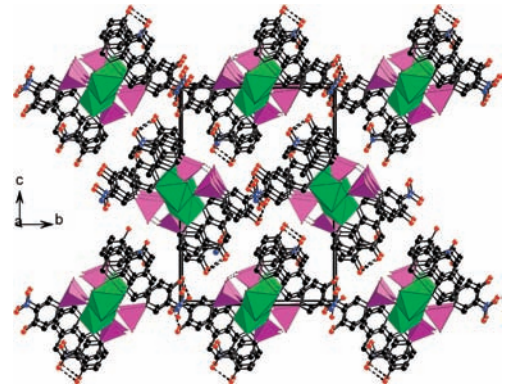

Figure 5. View of the structure of **3** down the *a* axis. The MnO_4N_2 octahedra and $CAsO_3$ tetrahedra are shaded in green and purple, respectively. N, O, and C atoms are drawn as blue, red, and black circles, respectively. Hydrogen bonds are drawn as dashed lines.

a 3D supramolecular network via weak van der Waals interactions (Figure 5).

Structure of $[M(phen)_2(H_2L^2)](ClO_4)\cdot(H_2O)$ (M = Mn, 4; Cd, 5). Compounds **4** and **5** are also isostructural; hence, only the structure of **4** will be discussed in detail as a representative. The asymmetric unit of **4** contains one manganese(II) ion, two phen ligands, one $\{H_2L^2\}^-$ anion, one perchlorate anion, and one lattice water molecule (Figure 6). The Mn(II) ion is octahedrally coordinated by two phenylarsonic oxygen atoms from two $\{H_2L^2\}^-$ anions and two bidentate chelating phen ligands. The Mn−O (2.077(3)−2.141(3) Å) and Mn−N (2.257(4)−2.348(4) Å) bond distances are comparable to those of **3** and those reported in manganese(II) phosphonates.[24]

Both the arsonate group and the hydroxyl group of the $\{H_2L^2\}^-$ anion are singly protonated, as indicated by a much longer As−O bond (Table 2). The arsenate ligand is bidentate and bridges with two manganese(II) ions via two of three arsenate oxygen atoms. The hydroxyl and nitro groups remain noncoordinated (Scheme 1c). A pair of Mn(II) ions are bridged by a pair of arsonate groups of two $\{H_2L^2\}^-$

(24) (a) Mao, J.-G.; Wang, Z.-K.; Clearfield, A. *Inorg. Chem.* **2002**, *41*, 2334. (b) Yang, B.-P.; Mao, J.-G. *Inorg. Chem.* **2005**, *44*, 5661. (c) Bao, S. S.; Chen, G.-S.; Wang, Y.; Li, Y.-Z.; Zheng, L.-M.; Luo, Q.-H. *Inorg. Chem.* **2006**, *45*, 1124. (d) Yin, P.; Gao, S.; Wang, Z.-M.; Yan, C.-H.; Zheng, L.-M.; Xin, X.-Q. *Inorg. Chem.* **2005**, *44*, 2761. (e) Merrill, C. A.; Cheetham, A. K. *Inorg. Chem.* **2007**, *46*, 278. (f) Ma, Y.-S.; Yao, H.-C.; Hua, W.-J.; Li, S.-H.; Li, Y.-Z.; Zheng, L.-M. *Inorg. Chim. Acta* **2007**, *360*, 1645.

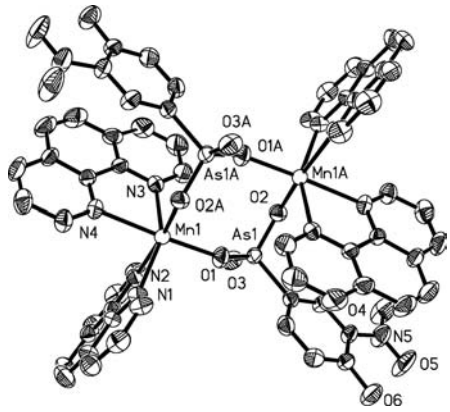

Figure 6. ORTEP representation of the metal arsonate dinuclear unit in compound **4**. The thermal ellipsoids are drawn at the 50% probability level. Symmetry code for the generated atoms: (a) $-x$, $-y + 1$, $-z + 1$. The perchlorate anion and lattice water were omitted for clarity.

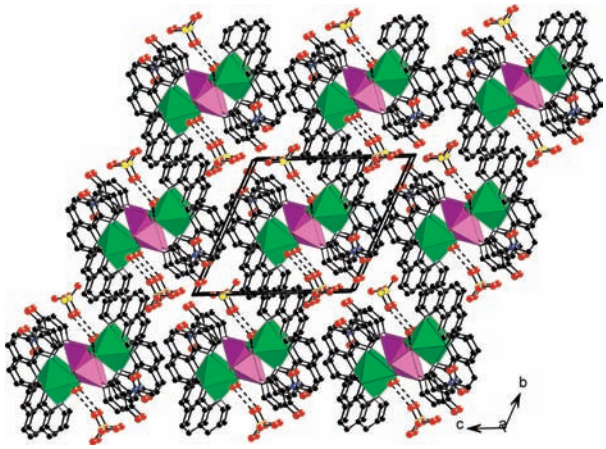

Figure 7. View of the structure of **4** down the *a* axis. The MnO_2N_4 octahedra and $CAsO_3$ tetrahedra are shaded in green and purple, respectively. N, O, C, and Cl atoms are drawn as blue, red, black, and yellow circles, respectively. Hydrogen bonds are drawn as dashed lines.

anions into a $[Mn_2(phen)_4(H_2L^2)_2]$ dinuclear cluster unit with a Mn_2As_2 four-member ring. The Mn···Mn separation within the $[Mn_2(phen)_4(H_2L^2)_2]$ dinuclear cluster unit of 4.880 Å is slightly shorter than that in compound **2**, in which two Mn(II) ions are interconnected by using the same Mn−O−As−O−Mn bridges, but much larger than that of two metal centers bridged by a pair of oxygen atoms (Mn−O−Mn bridge).

The discrete dinuclear clusters of compound **4** are assembled into a 3D supramolecular network via hydrogen bonds among noncoordination oxygen atoms of arsonate anions, perchlorate anions, and lattice water molecules as well as weak $\pi\cdots\pi$ packing interactions between neighboring phenyl or pyridyl rings of phen ligands or between the phenyl ring of the arsonate ligand and the phenyl ring of the phen ligand (Figure 7). The distances between the centers of these aromatic rings are in the range of 3.577−3.935 Å, and the corresponding dihedral angles are in the range of 0−10 °.

Structure of $[Mn(phen)_2(HL^1)](ClO_4)\cdot(H_2O)$ (6). Though compound **6** has a structural formula similar to those of compounds **4** and **5**, its structure is totally different. There is one unique manganese(II) ion in the asymmetric unit of **6** (Figure 8); it is octahedrally coordinated by two phenylarsonate oxygen atoms from two $\{HL^1\}^{-1}$ anions as well as two bidentate chelating phen ligands. The Mn−O (2.151(4)−2.153(4) Å) and Mn−N (2.257(5)−2.281(5) Å) distances are comparable to those reported in manganese(II) phosphonates[24] as well as in compounds **2** and **4**.

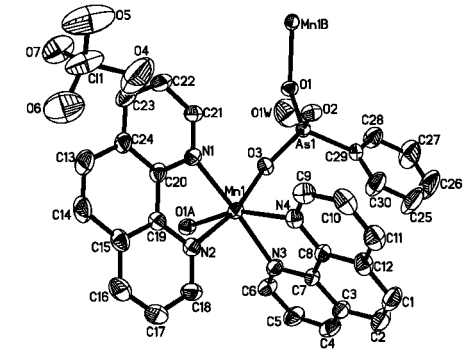

Figure 8. ORTEP representation of the selected unit in **6**. The thermal ellipsoids are drawn at the 30% probability level. Symmetry codes for the generated atoms: (a) $-x + 3/2$, $y + 1/2$, $-z + 1/2$. (b) $-x + 3/2$, $y - 1/2$, $-z + 1/2$.

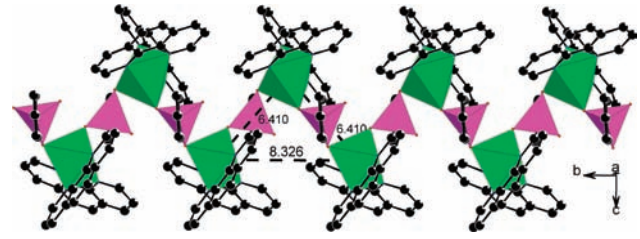

Figure 9. View of a 1D manganese(II) arsonate chain in **6** with labeling of some Mn···Mn distances. Mn, As, O, N, and C atoms are drawn as green, purple, red, blue, and black circles, respectively.

One oxygen atom of the phenylarsonate ligand is singly protonated, as indicated by an elongated As−O bond (Table 2). The phenylarsonate ligand is bidentate and bridges with two manganese(II) ions via two of its three phenylarsonic oxygen atoms (O(1) and O(3); Scheme 1d). Neighboring manganese(II) ions are bridged by $\{HL^1\}^{-1}$ anions into a 1D helical chain along the *b* axis (Figure 9). The Mn···Mn separations between two neighboring Mn(II) centers are 6.410(3) Å, and that between a metal center and its second nearest neighbor is 8.326(3) Å. The lattice water molecules and perchlorate anions are located at the cavities of the structure.

TGA Studies. TGA curves of compound **1** exhibit three main steps of weight loss (Figure 10). The first step started at 166 °C and was completed at 249 °C, which corresponds to the release of an aqua ligand and the water molecule formed by the condensation of two singly protonated arsenate groups. The observed weight loss of 4.95% is very close to the calculated value (5.05%). The second and third steps covering a temperature range of 265−754 °C overlapped, corresponding to the combustion of the phen and phenylarsonic ligands. The final product is assumed to be CdO. The total observed weight loss at 754 °C of 81.9% is close to the calculated value (81.7%). Compounds **2** and **3** are isostructural, and both of them exhibit two main steps of weight losses. The first one corresponds to the loss of a water molecule formed by the condensation of two singly protonated arsenate groups of two arsonate anions; the observed

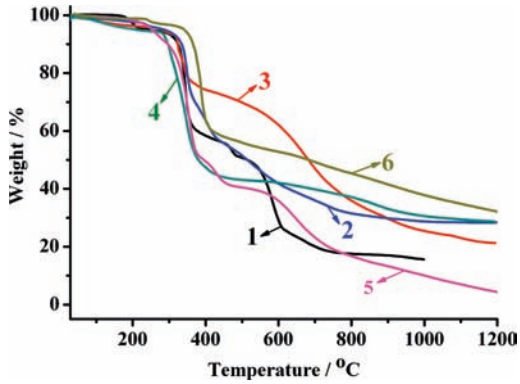

Figure 10. TGA curves of compounds **1**−**6**.

water losses of 2.1% for **2** (209−270 °C) and 2.2% for **3** (251−307 °C) are close to the calculated values of 2.3% and 2.2%, respectively. The second step (290−969 °C for **2** or 313−1096 °C for **3**) corresponds to the combustion of the phen and organo arsonate ligands. The final products are assumed to be a mixture of $M_3(AsO_3)_2$ (M = Mn or Cd) and As_2O_3 in a 1:2 molar ratio. The total observed weight loss (71% for **2** or 73.4% for **3**) is somehow larger than the calculated value (64.6% for **2** or 60.1% for **3**), which is probably due to the partial evaporation of As_2O_3 at high temperatures. Compounds **4** and **5** are also isostructural and exhibit similar TGA curves. Their TGA curves exhibit three main steps of weight loss, and the results of **4** will be discussed in detail as an example. The first step (52−240 °C) corresponds to the release of one lattice water and one water molecule formed by condensation of the two singly protonated arsenate anions, as in compounds **1**−**3**. The observed weight loss of 4.60% is very close to the calculated value (4.53%). The second step (260−485 °C for **4**) corresponds to the decomposition of the phen, ClO_4^- anion, and organo arsonate ligands. The third step corresponds to the further combustion of the arsonate ligands. The final residuals were not characterized due to their reaction with the TGA bucket made of α-Al_2O_3. TGA curves of compound **6** also exhibit three main steps of weight loss. The first step (67−335 °C) corresponds to the release of an aqua ligand and one water molecule formed by condensation of the two singly protonated arsenate anions, as in compounds **1**−**4**. The observed weight loss of 4.6% is very close to the calculated value (4.9%). The second weight loss occurring at 340−433 °C can be attributed to the decomposing of the perchlorate anion, phen, and arsonate ligand. The third step corresponds to further decomposition of the compound. The total weight loss at 1200 °C is 68%, and the final residuals were not characterized.

Luminescence Properties. The solid-state luminescence properties of compounds **1**−**6** as well as two free arsonate ligands were investigated at room temperature (Figure 11). The free phenylarsonic acid exhibits two fluorescent emission bands at λ_{max} = 323 and 368 nm upon excitation at 242 nm, whereas the free 4-hydroxy-3-nitrophenylarsonic acid displays a fluorescent emission band at λ_{max} = 421 nm with a shoulder band at 482 nm upon excitation at 237 nm (Figure 11a). The phen ligand displays a fluorescence emission band

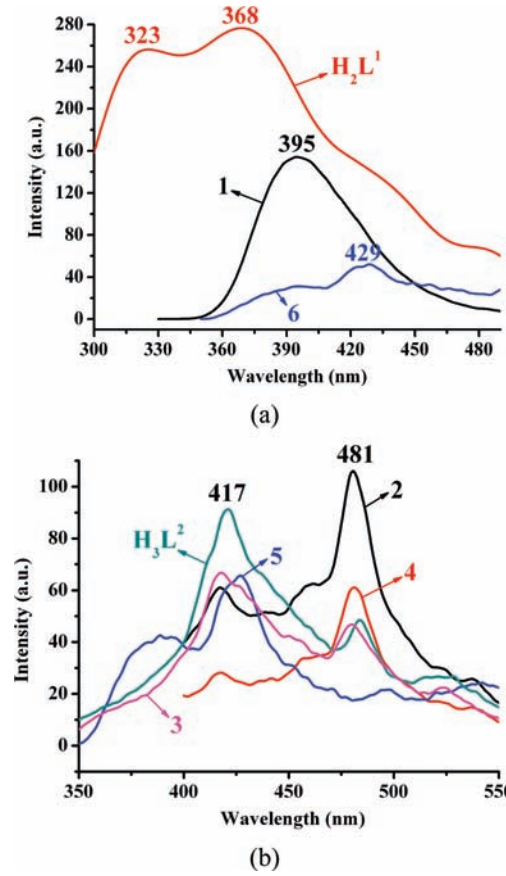

Figure 11. Solid-state emission spectra of compounds **1** (a), **2**−**5** (b), and **6** (a).

at λ_{max} = 381 nm with a shoulder band at 364 nm upon excitation at 339 nm.[25] For all three ligands, the chromophores are the aromatic rings, and the observed emission can be attributed to $\pi-\pi^*$ transitions. Compound **1** displays one strong broad emission band at λ_{max} = 395 nm (λ_{ex} = 300 nm), and compound **6** displays one very weak broad emission band at λ_{max} = 429 nm (λ_{ex} = 236 nm) upon complexion of both L^1 and phen ligands with the Cd(II) ion (Figure 11a). These emission bands are neither metal-to-ligand charge transfer nor ligand-to-metal charge transfer[26] in nature but, rather, can be assigned to an intraligand $\pi-\pi^*$ transition, which is similar to previously reported Cd−phosphonate−phen.[21d] Upon complexion of both L^2 and phen ligands with the Cd(II) ion, compounds **2**−**6** each displays one strong and one weak emission band at λ_{max} = 417 and 481 nm (λ_{ex} = 350 nm for **2**; λ_{ex} = 285 nm for **3**; λ_{ex} = 390 nm for **4**) and λ_{max} = 427 and 497 nm (λ_{ex} = 236 nm for **5**) (Figure 11b). These emission bands are also attributed to a ligand-centered fluorescence, as in compound **1**.

(25) (a) Adamson, A. W.; Fleischauer, P. D. *Concepts of Inorganic Photochemistry*; John Wiley & Sons: New York, 1975. (b) Yersin, H.; Vogler, A. *Photochemistry and Photophysics of Coordination Compounds*; Springer-Verlag: Berlin, 1987. (c) Zheng, S.-L.; Tong, M.-L.; Tan, S.-D.; Wang, Y.; Shi, J.-X.; Tong, Y.-X.; Lee, H.-K.; Chen, X.-M. *Organometallics* **2001**, *20*, 5319–5325. (d) Valeur, B. *Molecular Fluorescence: Principles and Applications*; Wiley-VCH: Weinheim, Germany, 2002.
(26) Perkovic, M. W. *Inorg. Chem.* **2000**, *39*, 4962.

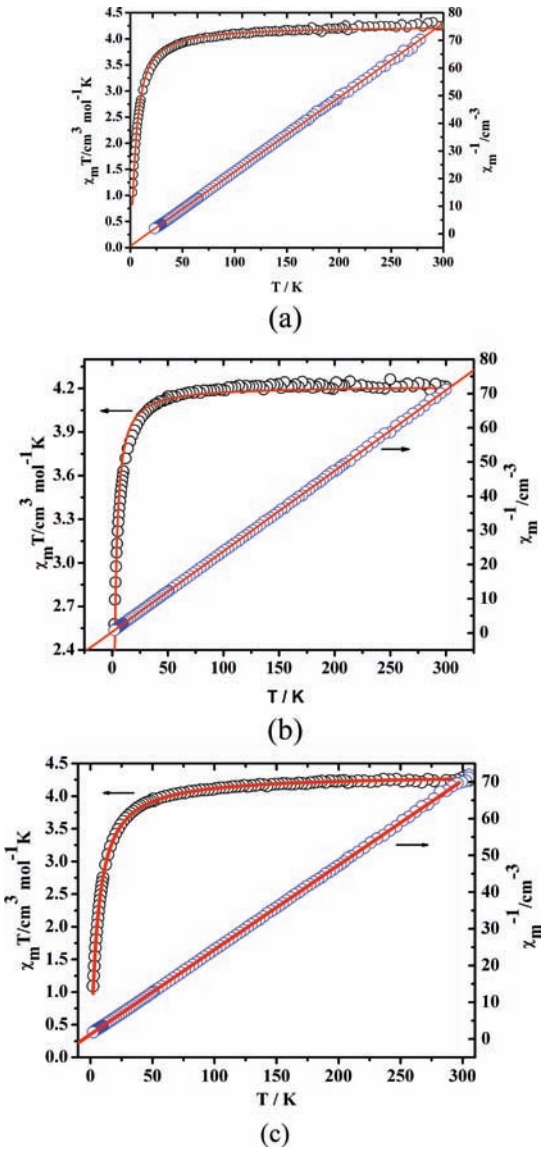

Figure 12. Plots of the $\chi_M T$ product and χ_M^{-1} versus T for compounds **2** (a), **4** (b), and **6** (c). The solid lines represent the best fit to the model with inclusion of the ZFS term.

Magnetic Property Studies. Temperature-dependent magnetic susceptibility measurements for compounds **2**, **4**, and **6** were performed over a temperature range from 2 to 300 K at 5 kOe. Fitting of the susceptibility data according to the Curie−Weiss law gives a Curie constant (C) of 4.1, 4.2, and 4.3 cm^3 K mol^{-1} for **2**, **4**, and **6**, respectively, and a Weiss constant (θ) of −5.1, −0.9, and −5.6 K for **2**, **4**, and **6**, respectively. The value of C is in good agreement with the expected one for one magnetically isolated Mn^{2+} ion with $S = 5/2$ per formula unit (4.24 cm^3 K mol^{-1}). At room temperature, the values of $\chi_M T$ are 4.25, 4.22, and 4.29 cm^3 K mol^{-1} respectively for **2**, **4**, and **6**. Upon cooling, the value of $\chi_M T$ decreases continuously and reaches a value of 1.06, 2.18, and 1.09 cm^3 K mol^{-1} respectively for **2**, **4**, and **6** at 2 K. Such behavior indicates the presence of weak antiferromagnetic interactions between the neighboring Mn^{2+} ions in all three compounds (Figure 12).

There are two types of Mn···Mn exchange pathways in compound **2**, namely through oxygen atoms (Mn−O−Mn) and arsonate groups (Mn−O−As−O−Mn) (Figure 4). The magnetic behavior of the compound is approximated by the contributions of the Mn^{2+} alternating chain.[27] The magnetic exchange interactions of such a chain can be described by the spin Hamiltonian $H = -J_1 \sum S_{2i}S_{2i+1} - J_2 \sum S_{2i+1}S_{2i+2}$,[27c] where J_1 and J_2 are the exchange coupling constants between the Mn^{2+} centers and the S values are classical spin operators. This approximation is justified for the manganese(II) ion, which exhibits a large spin ($S = 5/2$). The corresponding analytical expression for the χ product is given as follows (eq 1):

$$\mathrm{Mn{-}{-}Mn{-}{-}Mn\overset{J1}{-}{-}Mn\overset{J2}{-}{-}Mn{-}{-}Mn}$$

$$x = \frac{Ng^2\mu_B^2}{3kT}\left(\frac{1+u_1+u_2+u_1u_2}{1-u_1u_2}\right)$$

$$u_1 = \coth[J_1S(S+1)/(k_BT)] - [k_BT/(J_1S(S+1))]$$

$$u_2 = \coth[J_2S(S+1)/(k_BT)] - [k_BT/(J_2S(S+1))] \quad (1)$$

in which N, g, k, and β have their usual meanings. Fitting of the magnetic data using eq 1 gave a satisfactory result with superexchange parameters of $J_1/k_B = -1.16$ K, $J_2/k_B = -0.03$ K, and $g = 1.97$ (the agreement factor defined by $R = \sum(\chi_m T_{exp} - \chi_m T_{cal})^2/\sum(\chi_m T_{exp})^2$ is 3.8×10^{-4}). These values confirm the antiferromagnetic character of the magnetic interaction between the Mn^{2+} ions within the 1D chain.

It is noted that compound **4** contains a Mn_2 dimer, in which each pair of manganese(II) ions is interconnected via Mn−O−As−O−Mn bridges with much larger Mn···Mn separations (4.88 Å). The variable-temperature magnetic susceptibility data of the Mn^{2+} dimers for compound **4** were fitted according to the Hamiltonian $H = -2JS_1S_2$ with $S_1 = S_2 = 5/2$, as given in eq 2:[28]

$$\chi_d = \frac{Ng^2\beta^2}{kT} \times \frac{2e^{2x} + 10e^{6x} + 28e^{12x} + 60e^{20x} + 110e^{30x}}{1 + 3e^{2x} + 5e^{6x} + 7e^{12x} + 9e^{20x} + 11e^{30x}} \quad (2)$$

$$x = J/kT \quad (3)$$

in which N, g, k, and β have their usual meanings, and J is the exchange coupling constant between the two Mn^{2+} centers. Fitting of magnetic data using eq 2 gave a satisfactory result with the superexchange parameters of $J/k_B = -0.9$ K and $g = 1.96$ (with agreement factor R value of 5.9×10^{-4}). The obtained J value is comparable to the values reported for the other dinuclear manganese complexes.[29]

The magnetic behavior of compound **6** is approximated by the contributions of a Mn^{2+} infinite-helix-chain model of classical spins derived by Fisher with $H = -J \sum S_i \cdot S_{i+1}$.[29e] The corresponding analytical expression for the χ_{chain} and χ_m product is given as follows (eq 4):

(27) (a) Abu-Youssef, M. A. M.; Drillon, M.; Escuer, A.; Goher, M. A. S.; Mautner, F. A.; Vicente, R. *Inorg. Chem.* **2000**, *39*, 5022. (b) Cano, J.; Journaux, Y.; Goher, M. S. A.; Abu-Youssef, M. A. M.; Mautner, F. A.; Reiâ, G. J.; Escuer, A.; Vicente, R. *New J. Chem.* **2005**, *29*, 306, and references cited therein. (c) Cortés, R.; Drillon, M.; Solans, X.; Lezama, L.; Rojo, T. *Inorg. Chem.* **1997**, *36*, 677–683.

(28) Kahn, O. *Molecular Magnetism*; VCH Publishers, Inc.: New York, 1993.

$$\chi_{chain} = \frac{Ng^2\beta^2S(S+1)}{3k_BT}\frac{1+u}{1-u} = \chi_{mono}\frac{1+u}{1-u} \quad (4)$$
$$u = \coth[JS(S+1)/(k_BT)] - \{k_BT/[JS(S+1)]\}$$

$$\chi_m = \frac{\chi_{chain}}{1 - \frac{2zJ*\chi_{chain}}{Ng^2\beta^2}} \quad (5)$$

in which N, g, k, and β have their usual meanings, and J is the exchange coupling constant. Fitting of magnetic data using eqs 4 and 5 gave a satisfactory result with the superexchange parameters of $J/k_B = -0.38$ K, $zJ = -0.56$ K, and $g = 1.99$. The agreement factor R is 2.8×10^{-4}. These values confirm very weak intrachain and interchain antiferromagnetic magnetic interactions between the Mn^{2+} ions.

Conclusions

In summary, the syntheses, crystal structures, and luminescent and magnetic properties of six new manganese(II) or cadmium(II) arsonate compounds have been reported. Although the structurally characterized metal arsonates are very limited so far, some trends can be observed. It is noted that the metal arsonate is prone to exhibiting lower dimension structures under the presence of secondary phen ligand than the corresponding metal phosphonates. The arsonate group is more likely to be partially protonated and bridges with fewer metal centers even if phen is present; under similar conditions, the phosphonate ligands are usually fully deprotonated and are able to bridge with many more metal centers. This is also indicated by their pK_a values. According to the literature,[30] the pK_a values of the phenylphosphonic acid are 1.86 and 7.51, and the pK_a values of the phenylarsonic acid are 3.39 and 8.25, which means the second proton of the phenylarsonic acid is much more difficult to be removed than that of the corresponding phosphonic acid. Like phosphonate ligands, arsonate anions can also adopt various types of coordination modes. However, many more systematic works on metal arsonates are needed to fully understand their coordination chemistry and physical properties. Our future research efforts will be devoted to the studies of other transition metal or lanthanide arsonates.

Acknowledgment. This work was supported by the National Natural Science Foundation of China (Nos. 20825104 and 20521101), the NSF of Fujian Province (E0610034), Key Project of Chinese Academy of Sciences (No. KJCX2-YW-H01), and 973 Program (No. 2006CB932903).

Supporting Information Available: X-ray crystallographic files in CIF format and simulated and experimental XRD patterns and IR spectra for the six compounds. This material is available free of charge via the Internet at http://pubs.acs.org.

IC8016535

(29) (a) Fuller, A. L.; Watkins, R. W.; Dunbar, K. R.; Prosvirin, A. V.; Arifc, A. M.; Berreau, L. M. *Dalton Trans.* **2005**, 1891. (b) Ishida, T.; Kawakami, T.; Mitsubori, S.; Nogami, T.; Yamaguchi, K.; Iwamura, H. *J. Chem. Soc., Dalton Trans.* **2002**, 3177. (c) Durot, S.; Policar, C.; Pelosi, G.; Bisceglie, F.; Mallah, T.; Mahy, J. P. *Inorg. Chem.* **2003**, *42*, 8072. (d) Mukherjee, P. S.; Konar, S.; Zangrando, E.; Mallah, T.; Ribas, J.; Chaudhuri, N. R. *Inorg. Chem.* **2003**, *42*, 2695. (e) Fisher, M. E. *Am. J. Phys.* **1964**, *32*, 343.

(30) (a) Nagarajan, K.; Shelly, K. P.; Perkins, R. P.; Stewart, R. *Can. J. Chem.* **1987**, *65*, 1729. (b) Kina, K.; Tôei, T. *Bull. Chem. Soc. Jpn.* **1971**, *44*, 2416.